World Conference on
Timber Engineering
Oslo 2023

BEARING SUPPORTS REINFORCED WITH SCREWS: EXPERIMENTAL INVESTIGATION AND DISCUSSION OF THE DESIGN MODELS IN EUROCODE 5

Roberto Tomasi[1], Angelo Aloisio[2], Ebenezer Ussher[1], Kari Ryen Thunber[1], Eldbjørg Aaraas Hånde[1], Harald Liven[3]

ABSTRACT: This experimental investigation has been undertaken with the aim to discuss the current model for compression perpendicular to grain (CPG) proposed in the new Eurocode 5 draft. The current draft present two approaches proposed to assess load-carrying capacity of timber members subjected to CPG with reinforcement (Proposed reinforcement approach) and without reinforcement (New Model). The predictions of existing capacity models are compared to the experimental results of 39 timber specimens, distinguished by different load, screw and geometric configurations. Current capacity models for CPG with reinforcement assume two failure mechanisms, mainly characterized by their location, i.e. the contact area of the applied load (first mode) or the screw tips (second mode). However, the experimental tests reveal that the second mode never occurs despite the model predicting the occurrence of the second mode in more than half of the tested specimens. Additionally, the experimental tests show the fallacy of existing models in accurately estimating the capacity associated with the second failure mode. Parallelly, the model appears to be relatively conservative for the first failure mode.

KEYWORDS: Compression perpendicular to the grain, reinforcement with screws, experimental test

1 INTRODUCTION

The direction of the grain influences mechanical properties of wood, e.g. perpendicularly to the grain it presents considerable lower strength and stiffness [1]
Compression perpendicular to grain (CPG) failure leads to a collapse of the cellular tubes and acts as a failure transversely to the tubular layers.
Therefore, the CPG failure is a crucial problem, especially in the case of permanent deformation in the structures [2], even in the case when they do not cause structural failure.
In the case of CPG without reinforcement, the design approach proposed for the current draft of the new Eurocode 5 is based on the yield slip-line model, see Leijten [3].
Studies have also identified various techniques in improving the member strength in compression perpendicular to the grain (CPG) such as glued-in threaded rods and glued-on plywood plates. Alternatively, screws with uninterrupted threads have been observed to be economically viable in improving CPG capacity of timber members.
Therefore, the current draft of the consolidated version of the new Eurocode 5 on the table for discussion provides additional guidelines for implementing CPG with reinforcement [4].
The proposed design approach is based on the investigation made by Bejtka in 2005 [5], who observed three failure modes in timber subjected to CPG with reinforcement:

- the first failure mode is associated with pushing the reinforcing screws into the timber. It is observed with supports enhanced with short screws and the pushing-in capacity is assumed equal to the withdrawal capacity;
- the second failure mode occurs when slender screws are employed in reinforcing a member against CPG and it is characterised by buckling of the screws;
- the third failure mode is also associated with short screws in which a deformation is observed in a plane formed by the tips of the screws.

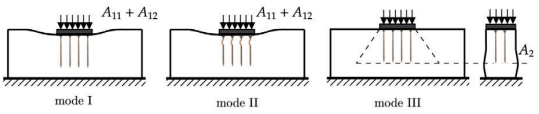

Figure 1: *Failure modes for CPG with reinforcements*

The minimum predicted value is considered to be the limit state to which the demand on a member in CPG may be compared for design. The candidate design approach still presents some gaps in knowledge concerning the test data that strengthen and validate the calculation model. Thus, Tomasi et al [6] experimentally investigated the CPG of

[1] Faculty of Science and Technology, Norwegian University of Life Sciences, P. O. Box 5003 Ås 1432, Norway
[2] Università degli Studi dell' Aquila, L'Aquila, 67100, Italy
[3] Moelven Industri, Norway

https://doi.org/10.52202/069179-0393

reinforced specimens, with the object of validating the standards approach, whose findings are summarized in this paper.

2 STANDARDS PROPOSAL

2.1 CGP WITHOUT REINFORCEMENT

The CPG model presented in [3] is based on the assumption that the compressive stresses spread as in an isotropic material with a degree depending on the deformations. The standard version of the model is given in Table 1.

Table 1: *Design model of non-reinforced members under CPG*

$$\sigma_{c,90,d} \leq k_p \cdot k_{c,90} \cdot f_{c,90,d} = B_1 \quad (1)$$

$$k_{c,90} = \sqrt{\frac{l_{ef}}{l_c}} \leq 4 \quad (2)$$

Where $k_{c,90}$ is a load arrangement factor, l_{ef} is the effective spreading length of the compressive stresses estimated by assuming a 45° diffusion angle, l_c is the contact length of the applied force, k_p takes into account the material behaviour and the deformation perpendicular to the grain (the factor accounts for the increased stiffness when the deformation increases).

2.2 CGP WITH REINFORCEMENT

Based on the failure modes described above, the capacity model proposed by Bejtka and Blass for CPG with reinforcement [7], is formulated as the minimum resistance associated with two following failure mechanisms (see Table 2):

- The first failure mode, labelled A_1, corresponds to the specimen failure by the contact area of the load. It is obtained by adding the timber and screw contributions, named A_{11} and A_{12} respectively. A_{11} accounts for the crushing of wood member at the support contact surface, adopting an effective length $l_{ef,1}$ higher than the contact length of the applied force, and k_{pr} for the material behaviour and the deformation perpendicular to the grain. A_{12} accounts for the pushing-in capacity of the screw including buckling effect.
- Second failure mode labelled A_2, considers failure of wood member with an effective length along a plane at the tip of the screws, which is determined adopting an effective length $l_{ef,2}$ calculated assuming a 45° diffusion angle.

The wood contribution A_{11} is coherent with the current guidelines in the Eurocode 5 for assessing unreinforced CPG in a member, which depends on the loading situation and the effective contact loading length due to the rope effect of contributing fibres adjacent to the loaded area.

Table 2: *Design model of reinforced members under CPG*

$$F_{c,90,Rk} = min\begin{cases} A_{11} + n \cdot A_{12} = A_1 \\ A_2 \end{cases} \quad (3)$$

where

$$A_{11} = k_{pr} \cdot b_c \cdot l_{ef,1} \cdot f_{c,90,k}$$

$$A_{12} = min\{F_{w,k}, F_{c,k}\}$$

$$A_2 = b \cdot l_{ef,2} \cdot f_{c,90,k}$$

$$l_{ef,1} = l_c + \min\{30\text{mm}, l_c\} + \min\{30\text{mm}, l_c, l_e\} \quad (4)$$

$$l_{ef,2} = l_r + (n_0 - 1) \cdot a_1 + \min\{l_r, a_{3,c}\} \quad (5)$$

The screw withdrawal strength can be calculated in function of the shear strength $f_{w,k}$ distributed along the screw surface areas according to this formula:

$$F_{w,k} = \pi \cdot d \cdot l_w \cdot f_{w,k}, \quad (6)$$

Where $f_{w,k}$ can be assumed as:

$$f_{w,k} = 8.2 \cdot k_w \cdot k_{mat} \cdot d^{-0.33} \cdot \left(\frac{\rho_k}{350}\right)^{k_\rho} \quad (7)$$

The screw buckling resistance is determined in function of an instability coefficient κ_c based on the model of a Winkler elastic beam in an elastic subgrade.

$$F_{c,k} = \frac{\gamma_R}{\gamma_{M1}} \cdot \kappa_c \cdot N_{pl,k} \quad (8)$$

where $N_{pl,k} = \pi \cdot \frac{d_1^2}{4} \cdot f_{y,k}$ and $\frac{\gamma_R}{\gamma_{M1}} \approx 1.18\ (*)$

*) $\frac{\gamma_R}{\gamma_{M1}}$ can be assumed equal to one for estimating the mean value of the buckling resistance.

3 EXPERIMENTAL CAMPAIGN

3.1 MATERIAL AND METHODS

The test specimens are glue-laminated timber of service class GL30 C, with dimensions of 800 × 140 × 225 or 1200 × 140 × 540 mm (length × width × height) with screw reinforcement produced by Rothoblaas and SFS. Figure 3 shows the considered load cases, tested with and without reinforcement, following the EN408 and ISO 6891 recommendations. The test procedure agrees with the one followed by Leijten [2], who investigated similar load cases without reinforcement.

Figure 2 show a schematic overview of the different screws, with the effective screw length applied in the design model. The screws are fully threaded self-tapping screws, except for the WT-T screw, which is double-threaded (in this case an effective screw length of 130 mm is used in the calculation). Each specimen is labelled with a unique name composed of its screw arrangement, screw

https://doi.org/10.52202/069179-0393

diameter, screw length, load case, and test number, see right Figure 2. All specimens were pre-drilled with a diameter 4.5 mm in a length of approximately 50 mm by using a bench pillar drill machine. The pre-drilling ensured having a straight hole, following the producer's recommendations for the diameter and length.
The screws are used in four arrangements according to Figure 4.

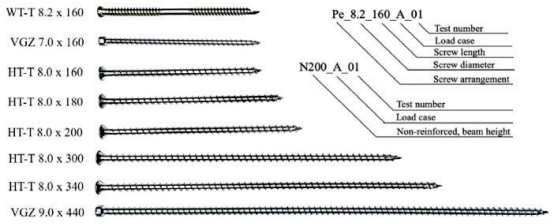

Figure 2: *Screws geometry and description of the labels for reinforced and non-reinforced test specimens.*

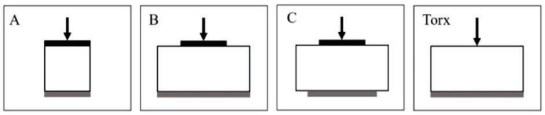

Figure 3: *Load cases*

It must be remarked that the experimental values cannot be compared with the characteristic resistance $F_{c,90,k}$ proposed in Equation (3). This is because the authors did not repeat each configuration multiple times to achieve a statistical description of the specific case. Therefore, an unbiased comparison with the experimental data requires estimating the predicted mean of the capacity. Hence, the mean of the resistance perpendicular to grain and yielding steel strength replaced the formulation's characteristic values in Table 2. The mean CPG timber strength is considered equal to $F_{c,90,m} = 3\,MPa$, following [8]. Conversely, the mean yielding strength of steel is set equal to 1000 MPa, based on separate experimental tests on the screws. The mass density of timber is assumed equal to $\rho_m = 390\ kg/m^3$. The load cases are graphically described in Figure 3.

- **Load case A** represents the block test of the specimens according to EN 408. For the reinforced samples, the predicted failure mode is the second, i.e. collapse by the screws' tips. Conversely, in the case of non-reinforced samples, the failure appears right below the load application area following to the first mode.
- **Load case B** considers a uniformly distributed load and corresponds to the case of the beam on continuous support (see left case in Figure 3).
- **Load case C** has direct loading on the opposite face. The support is a loading area of 140 x 180 mm (width x length). The goal is to investigate the failure in the reinforced area. Hence, the loading area is greater compared to the support (360 x 140 mm).
- **Torx:** This test directly loads the screw head and achieves the failure of the screw alone. The predicted failure mode is buckling for all screws, except for the shorter screws, where the effective screw length equals 130 mm. According to the theory of an elastic beam in elastic subgrade, the buckling capacity is not dependent on the screw length [9].

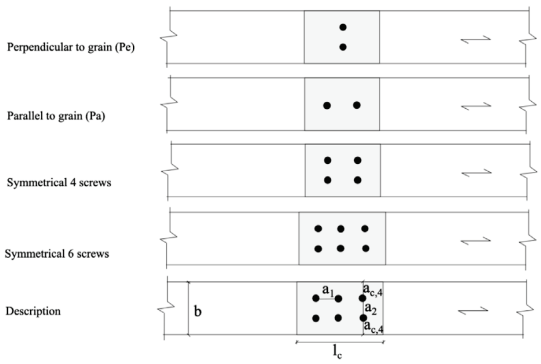

Figure 4: *Screw arrangement.*

3.1.1 Specimen preparation

The specimens were delivered as long beams by Moelven Limtre. The specimens were stored at the laboratory of wood technology at the material test laboratory of the Norwegian University of Life Sciences (NMBU). The relative humidity and the temperature during the storage are equal to 50% and 20° respectively. In a second step, the beams were cut into smaller pieces with a chainsaw to get the correct dimensions. The pre-drilling and insertion of the screw were done using electric drills produced by Bosch and Makita. The screws were drilled with a right angle, and the head was in all cases flush with the timber surface.

3.1.2 Testing procedure

The specimens are subjected to a compressive force by the load cell of the ZwickRoell Z1200 UTM (Universal Testing Machine). The deformation is measured by an integrated sensor in the load cell and external sensors. During the test execution, two horizontal and two vertical sensors are used, see Figure 5. The horizontal sensors are placed on each long side of the specimen corresponding to the screw tip. All estimations are carried out following EN408 and ISO6891 recommendations.

3.1.3 Loading protocol

There is no standard procedure for testing members subjected to CPG with screw reinforcement. However, the tests are executed on the basis of EN408 and ISO6891. In the ISO6891 procedure of loading the estimated load, F_{est} is determined as the minimum between A_1 and A_2. In the case of non-reinforced members for load cases B and C, the force is estimated with k_p equal to 1.0.
The test consists of four phases. Phases 1,2 and 3 are based on load rates, while the fourth is displacement-driven. Phases 1 and 2 follow the ISO6891 and aim to avoid residual initial deformations and stabilize the

https://doi.org/10.52202/069179-0393

loading area. The specimen is loaded up to 40% of the estimated resistance F_{est}, held for 30 seconds before the load decreases to 10% of F_{est}, and then held for 30 seconds. The load rate in phases 1 and 2 is determined as the ratio between 40% and 10% of F_{est} respectively, and 60 seconds. The actual load-displacement curves used in the analyses correspond to phase 3. Phase 3 follows the EN408. Hence, the maximum force will be reached within 300 ± 120 seconds. Phase 4 has a 1mm/min deformation rate, following Dietsch [10]. The test will stop automatically if the load reduces to 20% or the level of deformation reaches 12%.

In load cases A and Torx, the tests are executed with the first three phases, while load cases B and C are executed following the entire protocol. The Torx test is executed by connecting a Torx bit to the load cell through a steel plate. The mean moisture content of the specimens measured by a Delmhorts RDM3 instrument was 12.3%.

3.1.4 Estimation of the experimental capacity

The failure load for non-reinforced specimens has been estimated using an iterative procedure similar to the one described in EN 408 to estimate the compressive strength. Based on the load-displacement curves the line referring to the plausible elastic range between 10% and 40% of the estimated capacity is translate in a new parallel line, with 1% offset to the gauge length. The intersection between this second line 2 and the load-deformation curve determines the estimated capacity (F_{est}). If this value is within 5% of the predicted one $F_{c,90,est}$, it is considered valid. Otherwise, the process is repeated until the value is within the 5% tolerance.

3.2 EXPERIMENTAL RESULTS

he authors reported 31 tests with eight different screws in four loading conditions. The load-displacement curves exhibit an initial linear elastic behaviour, see Figure 5. The slope of the curves reduces when the load approaches the maximum load. After this point, the load decreases. This range corresponds to the failure of the screws and the local crushing of timber. After the screw failure, there is a slight increase in capacity after a certain point. This growth is related to the activation of the timber contribution. In the elastic range, the load-displacement curve has the same trend. Beyond the plastic range, the load-deformation curve depends on the specific failure mode. The horizontal expansion is below 2 mm for all cases, except for load case A, although it does not represent a design situation.

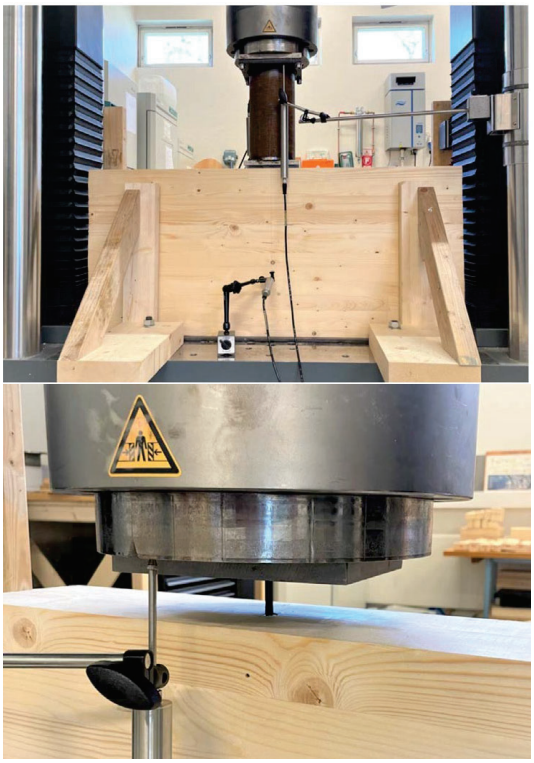

Figure 5: *Setup of specimen with height 540 mm in ZwickRoell Z1200- Setup of Torx test.*

Figure 6 plots all experimental results for load cases A (block test) B and C for the specimen with H = 225 mm, while Figure 7 plot the torx test results. The relevant experimental outcomes are resumed in ***Table 3*** and Table 4. The tables collects the test label, the failure mode, the maximum force (for torx test) and that corresponding to 1% deformation. The column 'increase' reports the percentage increment in capacity due to the presence of screws compared to the specimen without reinforcement.

The major aspects are:

Case A: The capacity increases slightly with the reinforcement. The observed failure mode is the timber failure, despite the significant deformation of the screws. The load-displacement curves are close to each other. As expected, the elastic stiffness of the reinforced model is higher. Theoretically, the effective diffusion length of the reinforced specimen is not fully exploited due to the specimen's geometry.

Case B: The failure modes are buckling and withdrawal. The horizontal displacement is below 1 mm for all cases, except for S6_7.0_160_B, where the horizontal displacement is 1.50 mm. Test Pa_7.0_160_B and Pe_7.0_160_B exhibited the same resistance at 1% deformation. The difference between the configurations is the screw arrangement. The curves of the reinforced specimens have a peak and then decrease, while those of the non-reinforced ones monotonically increase. As expected, the reinforcement causes a higher stiffness. The configuration S6_7.0_160_B shows a significant increase

in capacity. However, the configuration has a considerable number of screws, and the contact area is increased to 140 x 360 mm (width x length). For the configuration S6_9.0_440_B, the horizontal displacement is greater than 1 mm; otherwise, the horizontal displacement is below 1 mm. In the configurations with a 540 mm height, the predicted failure mode, A_1, is confirmed by the test results, except for S6_9.0_440_B. The capacity model yields a 20% overestimation of the test results. Interestingly, no differences emerged between the two configurations with different orientations of the screws (perpendicular or parallel to the grain direction). The predicted failure mode of the screws in the 540 mm specimen is buckling, except for the screw WT-T 8.2 x 160 mm, where withdrawal is reported.

In contrast to the predictions, all screws with a 160 mm length failed due to withdrawal.

In the case of 2 x HT-T 8.0 x 180 mm screws, the failure mechanism is both withdrawal and buckling.

4 x HT-T 8.0 x 180 mm has an apparent withdrawal failure. Similarly, HT-T 8.0 x 200 mm changes the failure mode with the number of screws. Considering a constant load area, the capacity variation between the load configurations may be due to screw length, diameters, and timber imperfections.

Case C: A steel plate with dimensions 360 x 140 mm (length x width) is applied on the non-reinforced side. The capacity of the test specimens increases with the reinforcement. The horizontal displacement is approximately 1-2mm for all cases. The configuration with 2x VGZ 7.0 x 160 mm had a higher capacity than 2 x WT-T 8.2 x 160 mm. The curves of reinforced specimens have a peak and then decrease. The capacity increases with the number of screws. For 225 mm specimens, the failure mode is withdrawal, despite the predictions. The distinction in capacity between A_1 and A_2 is minor.

Torx: The failure modes of the screws are withdrawal and buckling, see Figure 8. The load increases with the length of the screw, except when the size of the screw is 200 mm. In this case, the capacity decreases. All curves exhibit a clear peak. With the VGZ 7.0 screw, the capacity is higher compared to the HT-T 8.0 screw. However, the failure is reached at a smaller displacement. Contrary to the previously reviewed tests, the maximum force achieved is estimated. The predicted failure mode corresponds to the test results, except for VGZ 7.0 x 160 mm, where the failure mode is withdrawal. The design model's decisive capacity is consistently lower than the test results. The mean ratio between the test results and the predicted capacity is 1.55. The impact of the slenderness is considered by testing the HT-T screw with a constant diameter and different lengths. In all cases, the screw failed due to buckling.

3.3 DISCUSSION

The screw and timber contribution to the capacity of the reinforced specimens can be isolated using the outcomes of the Torx tests. Since the timber contribution in the Torx test can be assumed negligible, the Torx tests provide the contribution of a single screw. Accordingly, the role of timber can be estimated by subtracting from the force associated with 1% deformation the capacity obtained from the Torx test multiplied by the number of screws. The timber contribution to the capacity according to the failure mechanism A_1 , named A_{11}, reads:

$$A_{11} = \left(F_{1\%,def} - n \cdot F_{max}\right) \quad (9)$$

Parallelly, the average screw contribution to the capacity, named A_{12}, can be obtained from the $F_{\max}$ of the Torx tests as follows:

$$A_{12} = F_{max} \quad (10)$$

The main aspects emerging from the experimental results are the following:

- The timber contribution to the capacity of the reinforced specimen is approximately 73% and 51% for the samples with two and four screws, respectively. This fact proves that using four rather than two screws reduces the timber contribution by nearly 20%.
- The timber contribution moderately varies if the screw length increases from 160 mm to 440 mm. The A_{11} contribution is on average, 110 for 160 mm screws and 137 for 440 mm.
- The model significantly underestimates the screw contribution by 42% on average. Conversely, the disparity in terms of timber contribution is lower. On average, it is 2% for the two-screws specimens and -22% for the four screws. On the contrary, in this case, the design model overestimates the timber contribution for the four screws specimens. The mean timber contribution from test results is 72% and 51% with two and four screws, respectively. In the design model is 72% and 45%, with two and four screws.
- According to the standard proposal, k_{pr} should be 1.5 for load case B and 1 for load case C. Still, the experimental data contradict these assumptions. The test results for load cases B and C with identical screw arrangements (except for the size of the steel plates) are within the same range of capacity. The dissimilarity is insignificant and lower than 10% in most cases and on average 2%. Therefore, this fact proves that the capacity of the two load cases can be predicted with the same k_{pr} coefficient.

https://doi.org/10.52202/069179-0393

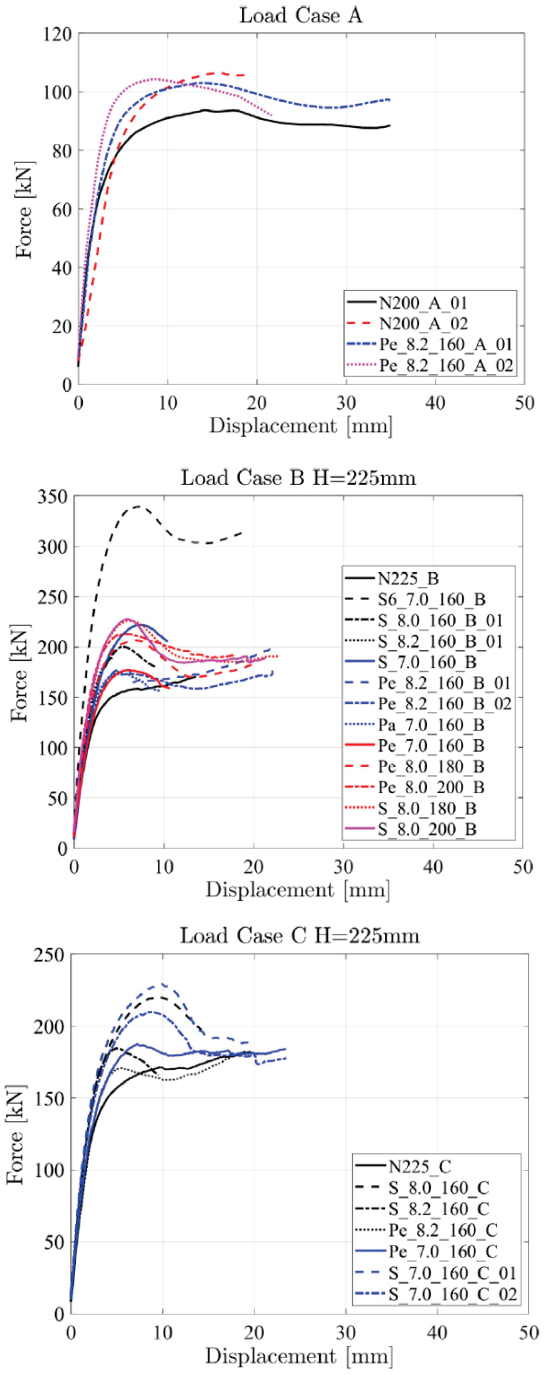

Figure 6: *Force–displacement curves for load case A, load case B, and load case C.*

Table 3: *Main results of the experimental tests and corresponding predictions according to the capacity model.*

Type			Failure mode	
	$F_{1\%,\,def}$	Incr.*	Exp.	Th.
	[kN]	[%]		
Load Case A				
N200_A	88	/	B_1	/
Pe_8.2_160_A	96	9.10	A_2	A_2
Load Case B				
N225_B	152	/	B_1	/
N540_B	182	/	B_1	/
Pe_7.0_160_B	172	13.20	A_1 $F_{w,k}$	A_2
Pa_7.0_160_B	172	13.20	A_1 $F_{w,k}$	A_2
Pe_8.2_160_B	174	14.50	A_1 $F_{w,k}$	A_2
Pe_8.0_180_B	196	28.90	A_1 $F_{w,k}$/ $F_{c,k}$	A_2
Pe_8.0_200_B	205	34.90	A_1 $F_{c,k}$	A_2
S_7.0_160_B	210	38.20	A_1 $F_{w,k}$	A_2
S_8.2_160_B	189	24.30	A_1 $F_{w,k}$	A_2
S_8.0_160_B	194	27.60	A_1 $F_{w,k}$	A_2
S_8.0_180_B	217	42.80	A_1 $F_{w,k}$	A_2
S_8.0_200_B	217	42.80	A_1 $F_{w,k}$	A_2
S6_7.0_160_B	311	104.6	A_1 $F_{w,k}$	A_2
Pe_8.0_300_B	234	41.40	A_1 $F_{c,k}$	A_1 $F_{c,k}$
Pe_9.0_440_B	230	39.40	A_1 $F_{c,k}$	A_1 $F_{c,k}$
Pa_9.0_440_B	225	36.70	A_1 $F_{c,k}$	A_1 $F_{c,k}$
S_8.0_300_B	256	55.20	A_1 $F_{c,k}$	A_1 $F_{c,k}$
S_8.0_340_B	271	64.20	A_1 $F_{c,k}$	A_1 $F_{c,k}$
S_9.0_440_B	292	77.00	A_1 $F_{c,k}$	A_1 $F_{c,k}$
S6_9.0_440_B	455	175.80	A_1 $F_{c,k}$	A_2
Load Case C				
N225_C	165	/	B_1	A_1 $F_{c,k}$
N540_C	182	/	B_1	/
Pe_7.0_160_C	173	11.60	A_1 $F_{w,k}$	A_2
Pe_8.2_160_C	169	9.00	A_1 $F_{w,k}$	A_1 $F_{c,k}$
S_7.0_160_C	192	23.90	A_1 $F_{w,k}$	A_2
S_8.2_160_C	183	18.10	A_1 $F_{w,k}$	A_2
S_8.0_160_C	191	23.20	A_1 $F_{w,k}$	
Pe_9.0_440_C	229	25.80	A_1 $F_{w,k}$	A_1 $F_{c,k}$
S_9.0_440_C	235	29.10	B_1	A_1

*) increase with respect to the unreinforced specimen

https://doi.org/10.52202/069179-0393

Table 4: *Main results of the experimental torx tests and corresponding predictions according to the capacity model.*

Type			Failure mode	
	F_{max}	F_{max}/A_1	Exp.	Th.
	[kN]			.
Torx test				
T_7.0_160	21.9	1.6	A_1 $F_{c,k}$	A_1 $F_{w,k}$
T_8.2_160	21.3	1.3	A_1 $F_{w,k}$	A_1 $F_{w,k}$
T_8.0_160	28.3	1.5	A_1 $F_{w,k}$	A_1 $F_{c,k}$
T_8.0_180	29.2	1.6	A_1 $F_{c,k}$	A_1 $F_{c,k}$
T_8.0_200	27.5	1.5	A_1 $F_{c,k}$	A_1 $F_{c,k}$
T_8.0_300	26	1.4	A_1 $F_{c,k}$	A_1 $F_{c,k}$
T_8.0_340	28.5	1.6	A_1 $F_{c,k}$	A_1 $F_{c,k}$
T_9.0_440	40.8	1.8	A_1 $F_{c,k}$	A_1 $F_{c,k}$

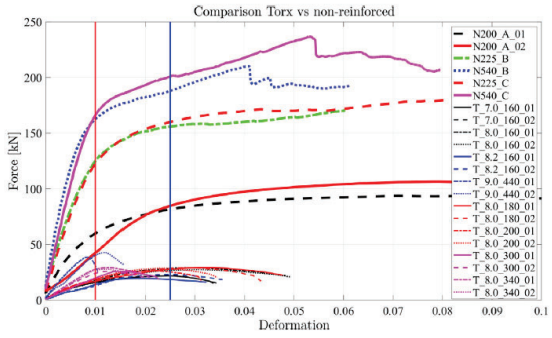

Figure 7: *Comparison between the torx tests on the single screws and those on non-reinforced specimens.*

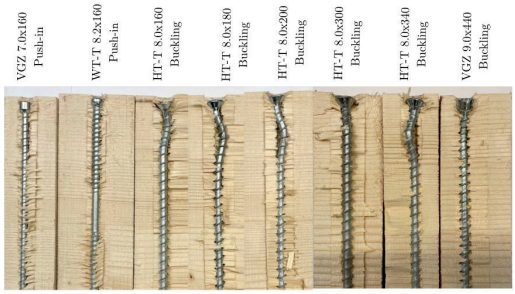

Figure 8: *Failure modes of the tested screws.*

Figure 9 plots the experimental capacity ($F_{1\%,def}$) and A_1, A_2 obtained from the design model. The most relevant aspect is that while A_1 and the experimental capacity are in good agreement, except for case C, A_2 is mostly lower than $F_{1\%,def}$ and exhibits a high scatter.

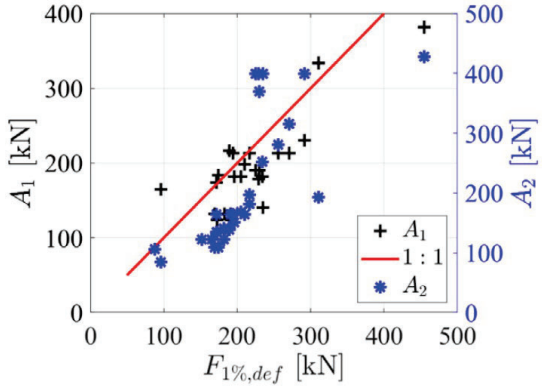

Figure 9:*. Experimental vs model predictions for the first (A1) and second (A2) failure mechanism,*

The failure mode achieved for all tests is according to A_1 for load cases B and C. However, some of the predicted failure modes appear to be different from the results of the experimental campaign. For example, in the event of shorter screws, the expected failure mode is mostly buckling, while the achieved failure mode is withdrawal. This evidence further proves that the specimen's failure corresponds to the A_1 mechanism. Additionally, it suggests that the A_2 model might be inaccurate and possibly underestimate the timber contribution by the screw tips. Consequently, it can be assumed that the capacity of A_2 is higher than the test results for load cases B and C. This fallacy possibly originates from the definition of the spreading length.

This failure mode A_2 is observed by Bejtka with small loading areas and short screws[5]. At the end of the screw, the force is transferred to the timber. The maximum pressure in the timber emerges at the screw tip and depends on the effective dispersion length and width. The effective length depends on the length of the screws, the screw arrangement, and the design situation.

This experimental outcome encourages researchers to study this aspect further to derive a reliable expression for the spreading length in predicting the capacity associated with the A_2 failure mechanism. Notably, the predictions for load case C are biased. The model underestimates the capacity, as a consequence of assuming $k_{pr} = 1$, as above remarked.

The timber contribution to resistance corresponds to the 1% deformation, while the screw contribution corresponds to the screw resistance, taken as the minimum between the buckling and the push-in resistances. However, this hypothesis is valid if the resistance of the screws is approximately reached at 1% deformation. Yet, the main difficulty behind this verification is the correct computation of the deformation in the Torx tests. While the specimen deformation in the non-reinforced specimens can be estimated as the ratio between the vertical displacement and the specimen height, this calculation might not be correct in the case of the Torx. During the push-in or buckling of the screws, the measured displacement does not result in the deformation of the entire specimen since only the

https://doi.org/10.52202/069179-0393

cylindrical layer wrapping the screw is affected by the deformation.

Therefore, the timber deformation associated with the Torx tests could be defined as the ratio between the vertical displacement and the screw length. Figure 7 compares the force-deformation curves of the non-reinforced and Torx tests, where the deformation in the non-reinforced specimens is computed as the ratio between the measured vertical displacement of the timber plate and the specimen height. The force-deformation curves of the non-reinforced samples are almost alike, showing a bend almost to the 1% deformation. The Torx tests exhibit a similar behaviour since the plastic branch approximately occurs between 0.01 and 0.02 deformation. Therefore, given the excellent estimation of the screw contribution A_{12} highlighted in the previous paragraphs, the authors conclude that the additivity hypothesis can be considered a reasonable assumption for a Standard. It must be remarked that the comparison in Figure 7 is only based on non-reinforced specimens to exclude all possible interaction phenomena occurring in the reinforced samples. The timber and screw contribution are already summed in the reinforced specimens. Thus, it is challenging to divide them and verify the additivity hypothesis.

4 CONCLUSIONS

This paper discusses experimental tests of timber specimens with screw reinforcement under compression perpendicular to the grain (CPG). In detail, the CPG tests comprise 31 structural arrangements different for the number and placement of the screws, specimens geometry and load pattern. The experimental capacities are used to validate the accuracy of the design model proposed in the next generation of Eurocodes. The experimental results show that using threaded screws as reinforcement effectively increases the capacity of timber subjected to CPG. However, the measured capacities do not entirely agree with the design model predictions. The current predictive model assumes two failure mechanisms, mainly distinguished by their location: the applied load's contact area (first mode A_1) or screw tips (second mode A_2). The first model is based on the mere summation of the timber and screw contributions. The failure modes achieved in the tests confirm the accuracy of the A_1. These tests ascertain the additivity hypotheses behind the predictive model. The experimental tests reveal that the second mode never occurs despite the model predicting the occurrence of the second mode in more than half of the tested specimens.

Conversely, the estimates corresponding to the failure mechanism A_1 agree with the test results. Yet, the predicted capacity is a bit lower for load case C. This might depend on the k_{pr} coefficient, assumed 1.5 and 1 for load cases B and C, respectively. The overall predicted failure mode of A_1 is mainly confirmed, except for the shorter screws.

The paper shows that the model predictions significantly improve if the same $k_{pr} = 1.5$ is assumed for all load configurations. Nonetheless, the additivity hypotheses for the A_1 failure mode can be considered sufficiently accurate for standards.

REFERENCES

[1] Porteous J, Kermani A. Structural timber design to Eurocode 5. John Wiley & Sons; 2013.

[2] Leijten AJM, Larsen HJ, der Put T. Structural design for compression strength perpendicular to the grain of timber beams. Constr Build Mater 2010;24:252–7.

[3] Leijten AJM. The bearing strength capacity perpendicular to grain of Norway spruce - Evaluation of three structural timber design models. Constr Build Mater 2016;105:528–35. https://doi.org/10.1016/j.conbuildmat.2015.12.170.

[4] Dietsch P. Reinforcement of timber structures - Standardization towards a new section for EC5. Proceedings of the 5th International Conference on Structural Health Assessment of Timber Structures (SHATiS) 2019, 25-27th September 2019.

[5] Bejtka I. Verstärkung von Bauteilen aus Holz mit Vollgewindeschrauben. Band 2 Der Reihe Karlsruher Berichte Zum Ingenieurholzbau, Doctoral Thesis, Fakultät Für Bauingenieur-, Geo- Und Umweltwissenschaften, Universität Fridericiana Zu Karlsruhe 2005;2. https://doi.org/10.5445/KSP/1000003354.

[6] Tomasi R, Aloisio A, Hånde EA, Thunberg KR, Ussher E. Experimental investigation on screw reinforcement of timber members under compression perpendicular to the grain. Eng Struct 2023;275. https://doi.org/10.1016/j.engstruct.2022.115163.

[7] Blass HJ, Bejtka I. Reinforcements perpendicular to the grain using self-tapping screws. Proceedings of the 8th World Conference on Timber Engineering 2004;1:233–8.

[8] Bogensperger T, Augustin M, Schickhofer G. Properties of CLT-panels exposed to compression perpendicular to their plane. At the Conference International Council for Research and Innovation in Building and Construction, Working Commission W18-Timber Structures 2011:1–15.

[9] Timoshenko SP, Gere JM. Theory of elastic systems 1961.

[10] Dietsch P, Rodemeier S, Blaß HJ. Transmission of perpendicular to grain forces using self-tapping screws. International Network on Timber Engineering Research INTER, Meeting 6, 2019.